FRACTAL DIMENSION OF THE STRANGE ATTRACTOR IN A PIECEWISE LINEAR TWO-DIMENSIONAL MAP

T. TÉL [1]
Fachbereich Physik, Universität Essen GHS, Postfach 103764, D-4300 Essen 1, Fed. Rep. Germany

Received 3 May 1983

We calculate the fractal dimension of the strange attractor in the map $x' = ax - \mathrm{sgn}(x) + bz$, $z' = x$. The method is based on the construction of the unstable manifolds of period-two points. The critical case characterized by heteroclinic tangents is investigated.

The fractal dimension [1,2] is a basic property of strange attractors. There have been several attempts for the estimation or numerical calculation of this quantity in different chaotic systems [3–12]. Since it has been recognized that for piecewise linear two-dimensional maps analytic calculations become possible [13–18], it is natural to search for an exactly solvable example among this type of maps.

The well-known transformation

$$x' = f(x) + bz, \quad z' = x, \tag{1}$$

describes a broad class of two-dimensional maps; with a quadratic f it reduces to the famous Hénon model [19,20]. The piecewise linear map specified by $f(x) = 1 - a|x|$ [13–15] shows in the structure of its invariant curves a topological similarity to that of the Hénon model [16–18]. For finding, however, a strange attractor the fractal dimension of which can be easily calculated, it is more convenient to consider the map defined by the function

$$f(x) = ax - \mathrm{sgn}(x), \tag{2}$$

where $\mathrm{sgn}(x)$ denotes the sign of x. Inspite of the fact that the one-dimensional ($b = 0$) limit of the two piecewise linear cases are quite similar, the two-dimensional extensions differ qualitatively. An essential new feature of the map associated with (2) is that its strange attractor consists of parallel straight line segments only (fig. 1a).

This property follows from the equations describing the invariant curves of periodic points of (1) [18]:

$$f^*_{i+1}(z) = f(z) + bf^{*-1}_i(z), \quad i = 1, ..., n. \tag{3}$$

They express that the invariant curve $x = f^*_i(z)$ around the period-n point G_i is mapped onto $x = f^*_{i+1}(z)$, the invariant curve around G_{i+1}, the next element of the n-cycle. In our case the fixed points $H_{1(2)}: (x^* = \pm(a + b - 1)^{-1}, x^*)$ lie outside the strange attractor (fig. 1b). They play a similar role as the fixed point H_- of the Hénon model [4] or of the piecewise linear map introduced by Lozi [13]. The period-two points $F_{1(2)}: (x_\pm = \pm(1 + a - b)^{-1}, -x_\pm)$, however, do belong to the strange attractor. Writing the branch of the invariant manifold going through $F_{1(2)}$ in the form

$$f^*_{1(2)}(z): \quad x = x_\pm + \lambda(z + x_\pm), \tag{4}$$

where the upper index belongs to f^*_1, we obtain from (3)

$$\lambda = a + b/\lambda, \tag{5}$$

which has two solutions

$$\lambda^{u(s)} = [a \pm (a^2 + 4b)^{1/2}]/2. \tag{6}$$

Restricting our considerations to the region $a > 1 - b$, λ^u (with the positive sign) is greater than 1, while $|\lambda^s| < 1$. Therefore, the branch with λ^u belongs to the unstable manifold of $F_{1(2)}$, while that with λ^s to the

[1] On leave from Institute for Theoretical Physics, Eötvös University, Budapest.

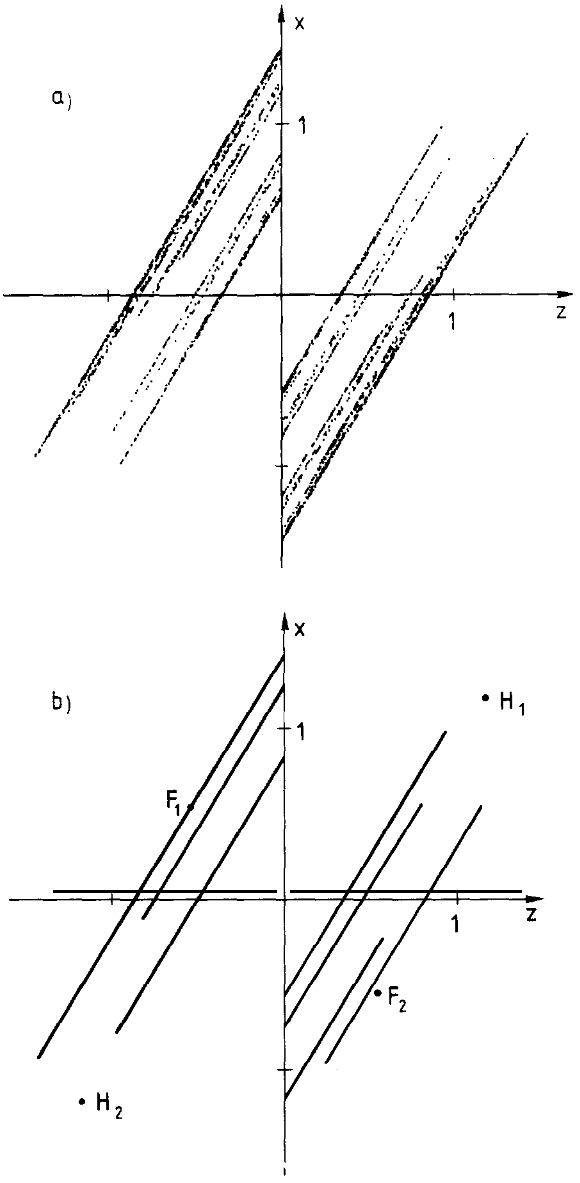

Fig. 1. (a) The strange attractor of map (1), (2) obtained in a numerical simulation after 3000 points. a = 1.35, b = 0.5. (b) The first branches of the unstable manifolds of F_1 as obtained after 3 steps of construction.

stable one. As the inverse of the first branch has a slope $1/\lambda$, eq. (3) generates new straight line segments with a slope $a + b/\lambda$, but, due to (5), this means that the new branches run parallel to the first one. A similar argumentation shows that the unstable (stable) manifolds of the fixed points and other periodic points, too, consist of straight line segments with slope λ^{u} (λ^{s}) only.

The strange attractor obtained in the computer simulation is related to the unstable manifolds of the period-two points. Fig. 1b shows a few branches of the unstable manifold of F_1 obtained by the method sketched above. It is an asymmetric object. Together with its inverted image, however, they give already a good approximation of the numerical result (fig. 2c). Similarly as in other cases [4,21,22], the strange attractor is expected to be the closure of the aforementioned unstable manifolds.

The construction makes it possible to calculate the fractal dimension of the strange attractor. We proceed as follows. The first branch going through F_1 intersects the x axis at $P_{1,0}$: (c^*, 0), where

$$c^* = (1 + \lambda^{\mathrm{u}})x_+ = 1 + c^*b/\lambda^{\mathrm{u}} , \qquad (7)$$

while that going through F_2 at $\overline{P}_{1,0}$: ($-c^*$, 0). We shall use the convention that $\overline{P}$ denotes the inverse of the point P, and $P_{i,n}$ stands for the nth image of $P_{i,0}$. The map (1), (2) is linear within one half-plane only, therefore, the validity of (4) is restricted to $z \leqslant 0$ in the case of f_1^* and to $z \geqslant 0$ in the case of f_2^*. The inverse functions are thus defined for $z \leqslant c^*$ and $z \geqslant -c^*$, respectively, and this means through (3) that the right endpoint of the branch going through F_2 is $P_{1,1}$: ($ac^* - 1$, c^*), while the left end-point of the other one is $\overline{P}_{1,1}$. Further steps do not create segments outside these branches (see fig. 2a–c), they are the outermost lines of the strange attractor. Starting with (4), eq. (3) generates two new branches $\overline{P}_{1,2}P_{2,0}$ and $\overline{P}_{2,0}P_{1,2}$, where the x-coordinate of $P_{2,0}$ is given by $1 - c^*b/\lambda^{\mathrm{u}}$, which form the innermost lines of the strange attractor. Thus, the region outside the band $P_{1,0}\overline{P}_{1,1}\overline{P}_{1,2}P_{2,0}$ and its inverted image cannot belong to the strange attractor. To find such a forbidden regime is essential in calculating the fractal dimension. It follows from (7) that the width of the bands is $2c^*b/[\lambda^{\mathrm{u}}(1 + \lambda^{\mathrm{u}2})^{1/2}]$, $q = b/\lambda^{\mathrm{u}}$ times the width of the parallelogram $P_{1,0}\overline{P}_{1,1}\overline{P}_{1,0}P_{1,1}$. Their area is $2c^{*2}b$, b times the area of $P_{1,0}\overline{P}_{1,1}\overline{P}_{1,0}P_{1,1}$, in accordance with the fact that the modulus of the jacobian of the map is b. The new branches generated by (3) in the next step intersect the x axis at $\pm[1 \pm (1 - c^*b/\lambda^{\mathrm{u}})b/\lambda^{\mathrm{u}}]$. Since the image of

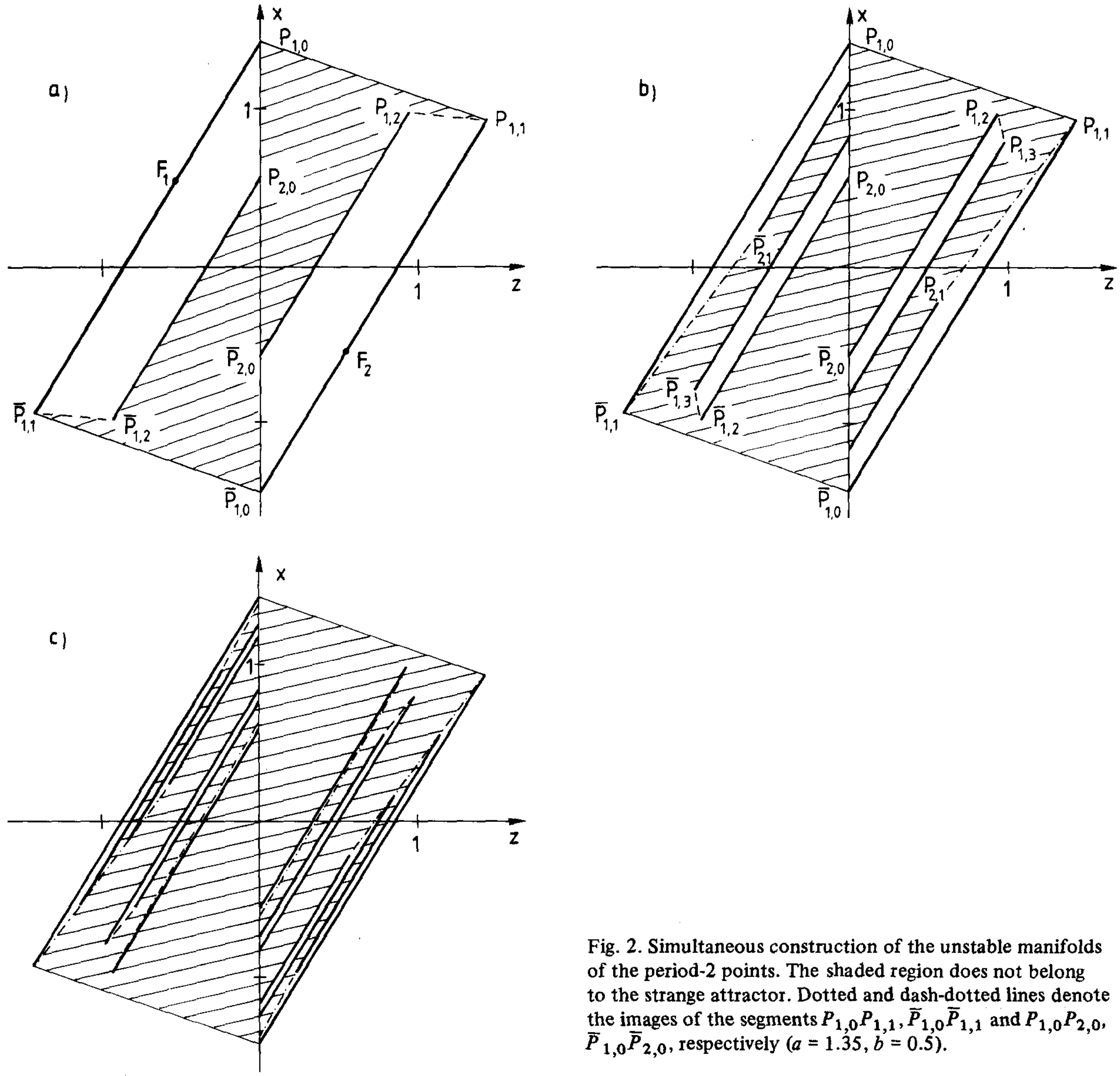

Fig. 2. Simultaneous construction of the unstable manifolds of the period-2 points. The shaded region does not belong to the strange attractor. Dotted and dash-dotted lines denote the images of the segments $P_{1,0}P_{1,1}$, $\bar{P}_{1,0}\bar{P}_{1,1}$ and $P_{1,0}P_{2,0}$, $\bar{P}_{1,0}\bar{P}_{2,0}$, respectively ($a$ = 1.35, b = 0.5).

the forbidden region is again forbidden, the bands covering the strange attractor after this step have a width $2c^*(1+\lambda^{u2})^{-1/2}q^2$ and an area $2c^{*2}b^2$. After n steps we shall have bands of width $2c^*(1+\lambda^{u2})^{-1/2}q^n$ and of a total area $2c^{*2}b^n$. Taking then small squares of side ϵ_n, $\epsilon_n \sim q^n$, the area can be covered by N_n such squares, where $N_n \sim (b/q^2)^n$. Thus, we obtain for the fractal dimension

$$d = \lim_{n\to\infty} \frac{\ln N_n}{\ln(1/\epsilon_n)} = \frac{2\ln[a/2+(a^2/4+b)^{1/2}] - \ln b}{\ln[a/2+(a^2/4+b)^{1/2}] - \ln b} . \tag{8}$$

For small values of b d behaves as $1 - \ln a/\ln b$.

We have to emphasize here that it does not follow from the argumentation that the fractal dimension of

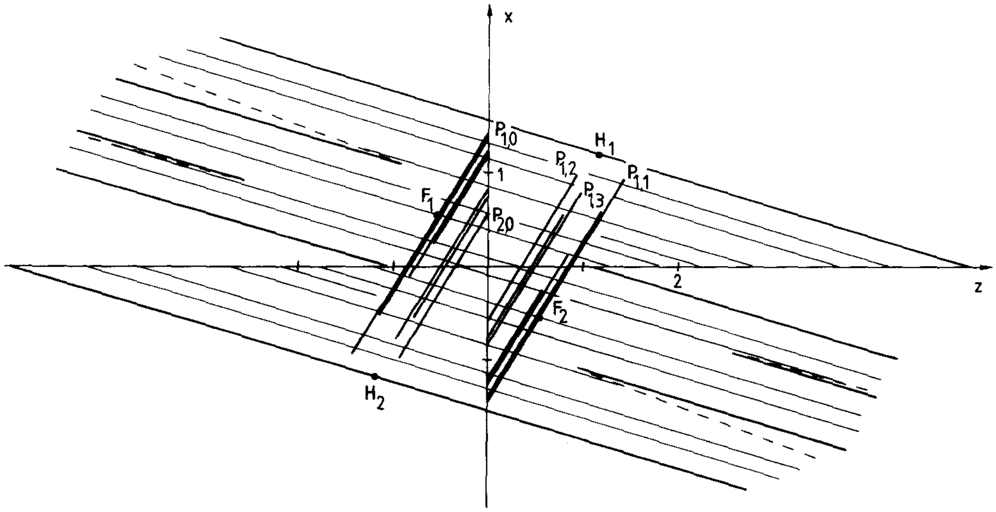

Fig. 3. Stable manifolds of the fixed points and of the period-2 points (thin lines) as obtained after 4 steps of construction. The dotted lines form parts of the preimages of the z axis. Homoclinic intersections with the unstable manifolds of the period-2 points can be observed. The parameters are as on figs. 1, 2,

a cross section of the strange attractor would be $d - 1$. A similar situation is expected in more general cases, too.

The stable manifolds can be constructed in an analogous way. As they are the unstable manifolds of the the inverted map which after the change $x \leftrightarrow -z$ is given by

$$x' = f(-x)/b + z/b, \quad z' = x, \tag{9}$$

the construction goes along the same lines as that discussed above but now (9) is to be used rather than (1). Fig. 3 shows the stable manifolds of the fixed points and period-two points, as well as, the strange attractor. The stable manifolds of the fixed points, similarly as that of H_- of the Hénon model or of the other piecewise linear case, determine the attracting region of the strange attractor.

By varying the parameters of the map, the structure of the strange attractor changes, and its fractal dimension is changed as well. Increasing a at a fixed value of b, a critical configuration is reached, at a certain a_c, where the points $P_{1,n}$ just touch the branch of the stable manifold of H_1 which goes through the fixed point. A straightforward calculation gives

$$a_c = 2(1 - b)^{1/2}. \tag{10}$$

Above a_c transverse heteroclinic points appear, the unstable manifolds of F_1, F_2 do not remain confined to the region defined by the stable manifolds of H_1, H_2, the strange attractor ceases to exist. The critical case $a = a_c$ has an important meaning. This corresponds to the two-dimensional extension of the diadic map (or Bernoulli shift) $x' = 2x \pmod 1$. It follows from (8) that, at a given b, the strange attractor possesses its greates fractal dimension at a_c. Fig. 4 shows $d_c \equiv d(a = a_c)$ as a function of b.

Finally, we note that in our case the Lyapunov

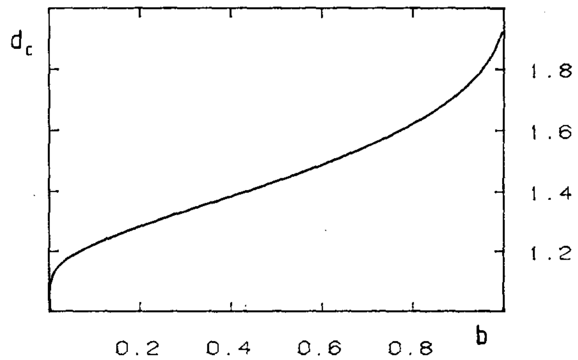

Fig. 4. The fractal dimension given by eq. (8) at $a_c = 2(1 - b)^{1/2}$ as a function of b.

numbers [4] of chaotic trajectories can be calculated easily since the strange attractor consists of parallel straight line segments only. They turn out to be $\Lambda_1 = \ln \lambda^u$ and $\Lambda_2 = \ln|\lambda^s|$, thus, the fractal dimension may be expressed as $d = 1 - \Lambda_1/\Lambda_2$ in agreement with the conjectures of Kaplan and Yorke [3] and Mori [5], which for two-dimensional maps coincide.

The author is indebted to Professor P. Szépfalusy for suggesting the investigation of discontinuous maps, and to Professor R. Graham for helpful discussions and the kind hospitality.

References

[1] B.B. Mandelbrot, Fractals: form, change, and dimension (Freeman, San Francisco, 1977).
[2] E. Ott, Rev. Mod. Phys. 53 (1981) 655.
[3] J.L. Kaplan and J.A. Yorke, Lect. Notes in Math. 730 (1979) 228.
[4] C. Simó, J. Stat. Phys. 21 (1979) 465.
[5] H. Mori, Prog. Theor. Phys. 63 (1980) 1044.
[6] H. Mori and H. Fujisaka, Prog. Theor. Phys. 63 (1980) 1931.
[7] D.A. Russel, J.D. Hanson and E. Ott, Phys. Rev. Lett. 45 (1980) 1175.
[8] H. Froehling, J.P. Crutchfield, D. Farmer, N.H. Packard and R. Shaw, Physica 3D (1981) 605.
[9] P. Grassberger, J. Stat. Phys. 26 (1981) 173.
[10] J.D. Farmer, Physica 4D (1982) 366.
[11] A.J. Chorin, J. Comp. Phys. 46 (1982) 390.
[12] C. Foias and R. Teman, Phys. Lett. 93A (1983) 451.
[13] R. Lozi, J. Phys. (Paris) 39 C5 (1978) 9.
[14] R. Lozi, in: Intrinsic stochasticity in plasmas, eds. G. Laval and D. Grésillon (Editions de Physique, Orsay, 1979) p. 373.
[15] M. Misiurewicz, in: Nonlinear dynamics (Ann. NY Acad. Sci. 357), ed. R.H.G. Helleman (The NY Acad. Sci., New York, 1980) p. 348.
[16] T. Tél, Z. Phys. B49 (1982) 157.
[17] T. Tél, Phys. Lett. 94A (1983) 334.
[18] T. Tél, Invariant curves, attractors and phase diagram of a piecewise linear map with chaos, to be published in J. Stat. Phys. 33 (1983).
[19] M. Hénon and Y. Pomeau, Lect. Notes in Math. 565 (1976) 29.
[20] M. Hénon, Comm. Math. Phys. 50 (1976) 69.
[21] P. Holmes, Philos. Trans. R. Soc. A292 (1979) 419.
[22] Y. Ueda, J. Stat. Phys. 20 (1979) 181.